A New Test Specimen for Self-Restraint Solidification Crack Susceptibility Test of Electron-Beam Welding Bead†

— Fan-Shaped Cracking Test —

Fukuhisa MATSUDA* and Kazuhiro NAKATA**

Abstract

A new self-restrained hot cracking test specimen used for the evaluation of the solidification crack susceptibility of electron-beam weld bead was proposed in this report, as a result of the investigation for cracking mechanism of weld bead with higher welding speed in Houldcroft-type test. The shape of the new test specimen was spreaded out like an unfolded fan, named as "Fan-shaped test", as welding proceeded. The dimensions of the test specimen were determined for aluminum alloys and stainless steels. Then the solidification crack susceptibilities for twelve different aluminum alloys and four stainless steels were compared and investigated.

KEY WORDS : (Hot cracking) (Hot cracking test) (Solidification) (Electron-beam welding) (Aluminum alloy) (stainless steel)

1. Introduction

As electron-beam welding (EBW) is usually done with a high energy density and high welding speed without any filler wires, the feature of the weldment has narrow widths of fusion zone and HAZ in addition to deep penetration. Accordingly, the susceptibility to solidification cracking in weld bead with EBW is generally lower than with conventional arc welding.

Therefore when usual self-restrained solidification crack susceptible tests used in arc welding, for example Houldcroft test, are applied to EBW as they are, the solidification crack does not appear in the weld bead in general. However the solidification cracks are often seen in the actual welded joints with EBW for aluminum alloys, austenitic stainless steels, high nickel alloys and so on.

The authors have thought that the shape of self-restrained cracking test specimen for EBW weld metal is a little different from that for arc welding. Therefore the authors tried to develop a new test specimen for self-restrained solidification cracking test appropriate for EBW weld bead, taking into consideration the principles of initiation and propagation of solidification cracking in Houldcroft-type test which reported in the previous report[1] .

Consequently the authors have reported here the shape and dimension of the test specimen recommended for evaluation of solidification crack susceptibility for EB—weld bead of aluminum alloys and stainless steels, respectively.

A part of this investigation was reported by the authors in a short note[2] .

2. Qualitative Consideration on Shape of New Test Specimen

Houldcroft cracking test[3] , which is commonly called" Fishbone Test" , is well known as a simple self—restrained solidification crack susceptible method of weld bead with GTA welding for thin sheet. Also, a mechanism of cracking for Houldcroft test was theoretically investigated[4] .

However, for electron-beam weld bead having a narrower weld bead, Houldcroft test as it is is not suitable for solidification crack susceptible test method, because there is often no cracking in the weld bead. The main reason why the crack is not observed in the weld bead is considered that solidification crack does not initiate at starting point of the weld bead (ie, specimen edge). In order to make a solidification crack at the starting point of such an electron-beam weld bead, the width of specimen edge should be considerably reduced.

Moreover, according to the investigations by Ando et al[5] and the authors in the previous report[1] , the cracking test specimen for a higher speed of welding was recommended to have a shape of the reversed Houldcroft-type that the specimen width increased with an advance of welding for the purpose of ceasing

† Reseived on September 30, 1982

* Professor

** Research Associate

Transactions of JWRI is published by Welding Research Institute of Osaka University, Ibaraki, Osaka, Japan

of a propagating crack.

The authors qualitatively describe in the following on the principles of initiation, propagation and ceasing of solidification cracking in weld bead in order to explain the remarkable difference on the test specimen shape.

(1) Initiation of crack; When welding is started along centerline of specimen from the end of specimen(S) as shown in **Fig.1 (a)** (i), a sudden thermal expension (Exp.) of weld bead and HAZ generates along the weld line in the starting area .Consequenty as in **Fig.1 (a)** (ii) a solidification crack initiates due to high rate of tearing strain(Y−Y') introduced by rapid thermal expansion of weld zone in the specimen whose temperature gradient vertical to weld line is considerably high.

The crack will not occur in principle both **Ws** is too wide or too narrow because of an excess restraint due to wide specimen width against opening deflection force(R−R') in the former and of a less deflection force due to lacking of temperature gradient vertical to weld line in the latter.

Therefore there is the optimum **Ws** for each metal, welding condition and weld bead width which easily initiates the solidification crack at the specimen edge. Dimension of **Ws** in electron-beam welding with a higher speed and narrower weld bead is generally considered to be narrower than that in GTA welding.

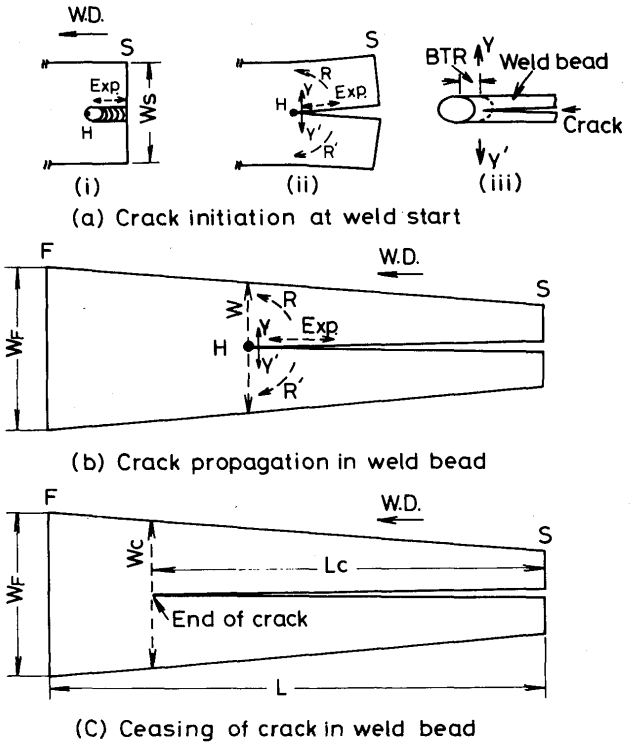

Fig. 1 Qualitative explanation of mechanism of solidification cracking

Therefore the optimum **Ws** should be experimentally decided for each metal.

The tip of the crack is existing within Brittleness Temperature Range(BTR) in succession to the molten puddle and propagating with advance of welding as shown in **Fig.1** (1) (iii) as long as the amount of the rate of tearing strain (Y−Y') exceeds the limit of the critical strain rate required to cause cracking (CST)[6] of solidifying metal.

(2) Propagation and ceasing of crack; In **Fig.1** (b) the solidification crack continues to propagate as the rate of tearing strain in BTR introduced by the difference between the opening deflection force caused by the thermal expansion and the restraint force corresponding with the specimen width **(W)** at instantaneous location of weld bead is exceeding the limit of the critical strain rate. However in Fig.1 (b), the restraint force is gradually increased with an advance of welding due to increase of specimen width. Finally when **W** reaches **Wc** (Critical Width) as welding proceeds, the propagating crack ceases as shown in **Fig.1** (c). The welding continuously proceeds to the other end of specimen whose width is $\mathbf{W_F}$. Therefore the solidification crack susceptibility of the specimen is represented by the factors of **Wc, Lc, Lc/L** and so on. The longer the **Lc** in the same specimen size, the higher the crack susceptibility is. Therefore the experimental decision for dimensions of $\mathbf{W_F}$ and **L** besides **Ws** are required to develop the cracking test specimen.

3. Test Specimen for Aluminum Alloys

3.1. Materials and welding procedure used

The materials used were 6mm (partly 6.5mm) thick 12 different types of commercial aluminum alloys. Chemical compositions of these alloys are listed in **Table 1.** Sciaky vacuum EBW machine of 60kv max. in accelerating voltage and 500mA max. in beam

Table 1 Chemical compositions of commercial aluminum alloys used

Material	Chemical composition (wt%)								
	Si	Fe	Cu	Mn	Mg	Cr	Zn	Ti	Zr
1100-H112	0.01	0.57	0.13	0.01	0.01	Tr	0.01	0.01	-
2017-T6	0.27	0.27	4.09	0.48	0.48	0.01	0.02	0.01	-
2219-T87	0.08	0.11	6.32	0.33	0.01	0.01	0.04	0.04	0.14
3003-H112	0.18	0.64	0.13	1.10	0.01	Tr	0.02	0.02	-
5052-H112	0.10	0.24	0.06	0.02	2.47	0.22	0.01	0.02	-
5083-H112	0.14	0.19	0.02	0.64	4.55	0.12	0.02	0.02	-
6061-T5	0.57	0.16	0.18	0.04	0.89	0.09	0.10	0.02	-
6063-T5	0.45	0.19	0.02	0.02	0.56	0.01	0.02	0.01	-
6N01-T5	0.78	0.19	0.02	0.20	0.52	0.01	0.06	0.02	-
7N01-T5	0.07	0.18	0.10	0.46	1.15	0.20	4.50	0.02	0.14
7003-T5	0.07	0.18	Tr	0.14	0.73	0.09	5.54	0.02	0.14
7075-T6	0.10	0.19	1.64	Tr	2.62	0.19	5.62	0.02	-

current was used through this investigation. EB welding was done without any fixtures for aluminum alloys.

3.2 Shape and dimension of test specimen

(1) Dimension of **Ws** *at welding start*

The first experiment is to decide the specimen width at the edge of test specimen **(Ws)** from which the solidification crack occurs at the start of welding bead by EBW. As illustrated in the sketch in **Fig.2,** the full-penetrated beads with EBW were made parallel to the plate side for 6061, 2017 and 5052 alloys, on the distance of (1/2)**Ws** apart from one side of the plate (100mm in width x 200mm in length x 6mm in thickness). Then the dimension of (1/2)**Ws** was varied from 5 to 100mm in this experiment. The most important thing is that a full-pentration welding is completed from the start of welding bead. In order to complete this purpose the plate thickness of the specimen at the starting edge was a little reduced in back side to about 3mm as shown in Fig.2, though the welding condition for 6mm thick plate was applied to it.

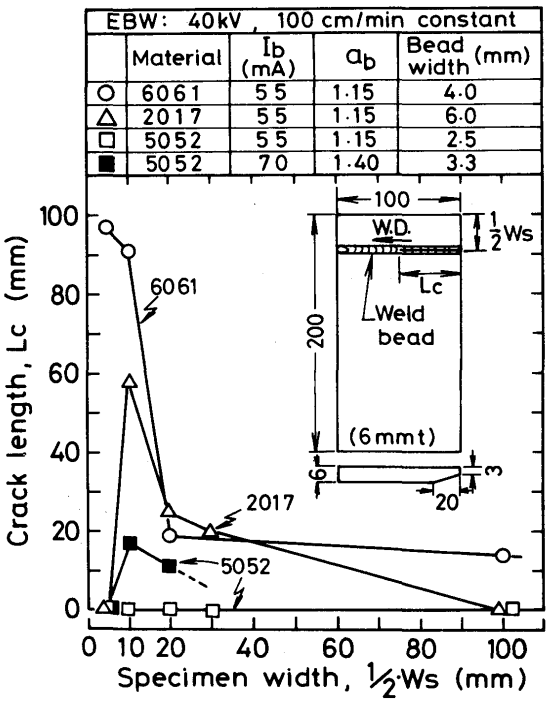

Fig. 2 Investigation of specimen width, (1/2)**Ws**, required to cause crack initiation and to keep crack propagation for aluminum alloys

In Fig.2 the relation between (1/2)**Ws** of specimen width and crack length on the specimen for 6061,2017 and 5052 alloys was shown. The focal point of electron-beam shown in *a*b value was upside the plate surface, which was not the minimum bead width, and welding speed was 100cm/min.

As shown in Fig.2 the dimension recommended for (1/2)**Ws** which surely initiated the solidification crack in the weld bead was about 10mm in width though there was no crack in the weld bead of 5052 plate in 55mA of beam current. Moreover, more detailed investigations were done on the effect of weld bead width in variation of *a*b on crack initiation at the specimen edge. The results are shown in **Fig.3 (a), (b)** and **(c)** for 6061, 2017 and 5052 respectively. The increase of the weld bead width clearly increased the crack susceptibility for each alloy at the same specimen width. For 5052 a repeated experiment with 1.15 of *a*b showed the initiation of a short crack for 10mm of (1/2)**Ws** as shown in Fig.3 (c). Moreover, the

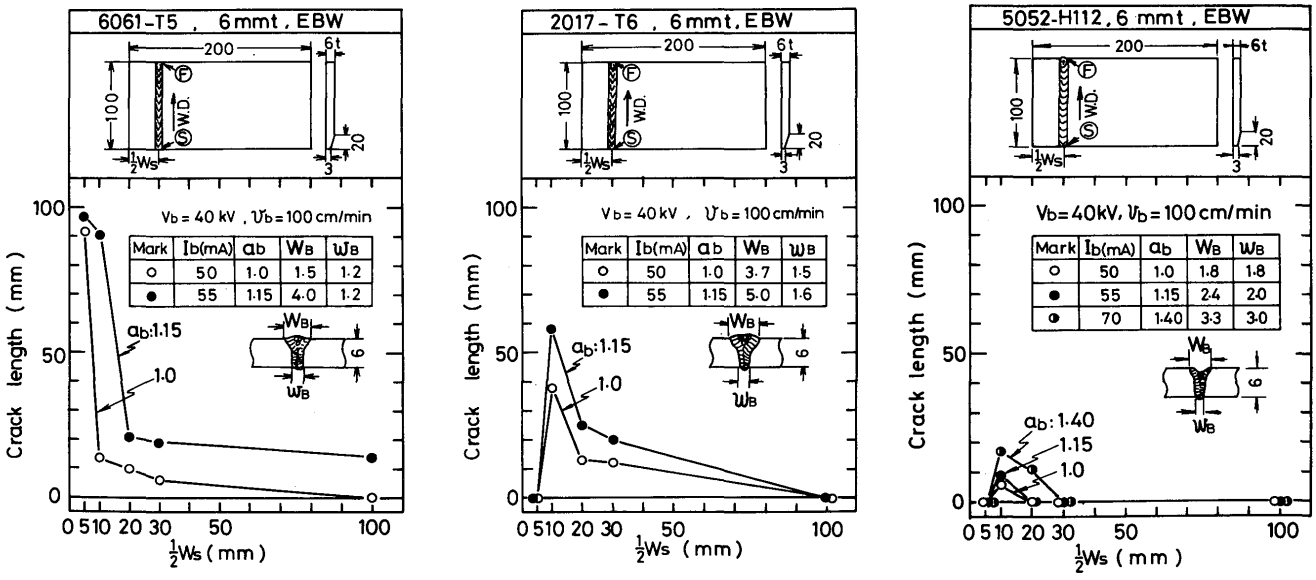

(a) 6061 alloy (b) 2017 alloy (c) 5052 alloy

Fig. 3 Effect of weld bead width in variation of focal point on feasibility of crack initiation at specimen edge

capability of crack initiation was shown in much narrow bead by 1.0 of ab.

As a result of these experiments the authors have recommended that the dimension in specimen edge is to be 20mm for **Ws** for aluminum alloys.

(2) Dimensions of L and W_F

The second experiment is to decide the dimensions of specimen length(**L**) and width at the end of specimen(W_F) or expanding angle. From the restriction of welding vacuum chamber size the specimen length was selected to 200mm for **L**. Therefore the effect of dimension of W_F on crack length in test specimen was investigated using the shape in Fig.1(c)specimen of 20mm for **Ws** and 200mm for **L**.

The results of crack susceptibility (length) for 6061 and 5052 alloys are shown in **Fig.4**. On vertical axis the crack susceptibility is represented by the ratio of crack length on surface to a whole bead length of 200mm(= **L**). The scattering in data was seen small enough. As the cracking occurred over a whole bead length for 40mm W_F for 6061, W_F more than 40mm was required to evaluate the crack susceptibility. From the result of about 80% in crack susceptibility of 6061 which is one of the most crack susceptible alloys the authors have recommended the dimension of 60mm as W_F for the specimen length of 200mm.

Subsequently the authors investigated the necessity of the fins for the test specimen which are usually provided in Houldcroft–type specimen. **(A)**, **(B)** and (**C**) in **Fig.5** show respectively three different specimen shapes without fins, with short fins and with long

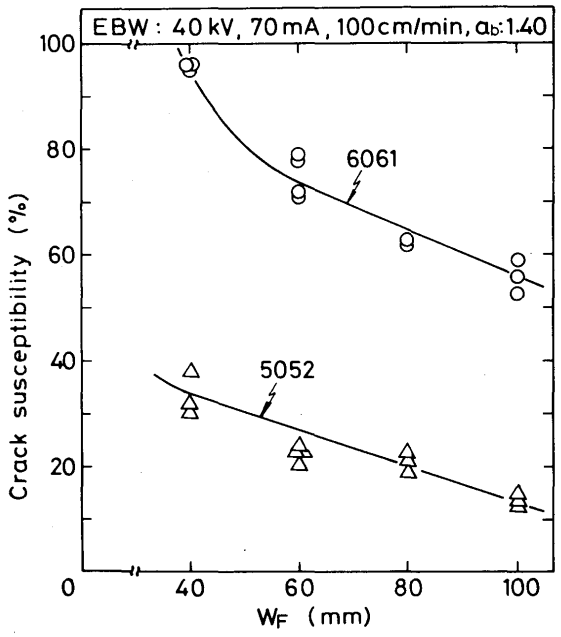

Fig. 4 Effect of width at the end of specimen, W_F, on crack susceptibility of weld bead for 6061 and 5052 alloys in specimen length of 200mm

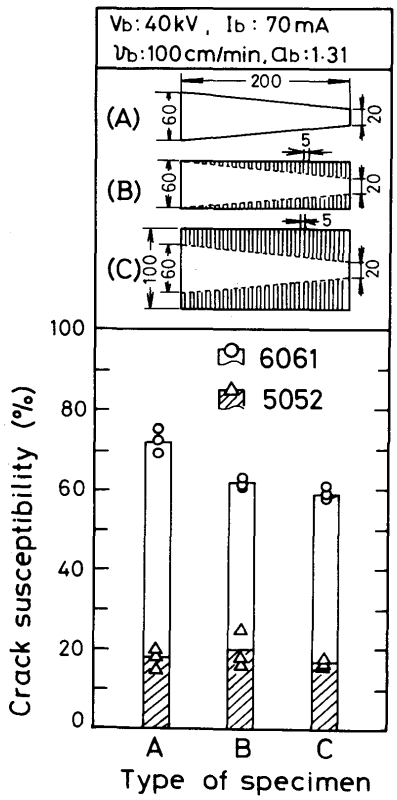

Fig. 5 Effect of addition of fins to test specimen on solidification crack susceptibility for aluminum alloys (welding speed of 100cm/min)

fins for the wider specimen width. The results tested are shown for 6061 and 5052 alloys.

The difference in crack susceptibility was seen only in (A) of 6061 but not so clear in this experiment for 100cm/min of welding speed. Of course in lower welding speed the difference will be much clear, but the experiments as 100 cm/min or more the fines will be unnecessary even for aluminum alloys of high thermal conductive metal.

Therefore the shape and dimension of the self-restrained cracking test specimen was experimentally defined for higher welding speed as 100cm/min of electron-beam welding for 6mm thick aluminum alloys as shown in Fig.6.

3.3 Comparion of crack susceptibility for various aluminum alloys

Now the authors have compared the solidification crack susceptibility of twelve different 6mm (partly 6.5mm) thick aluminum alloys using the new test specimen as in **Fig.6.** Test results are collectively shown in **Fig.7.** The welding condition was basically constant in 40KV–100cm/min–ab1.40, but varied 70 to 85mA in beam current depending upon the type of alloy as shown in the upper of Fig.7. The bead width

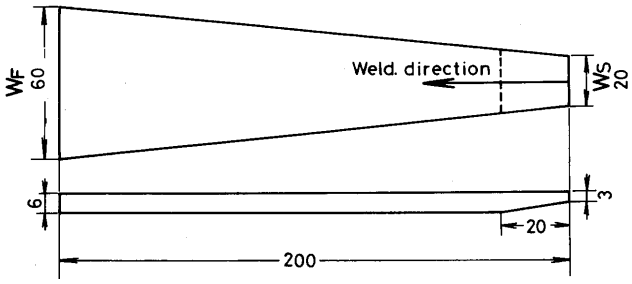

Fig. 6 A new crack susceptible test specimen recommended for electron-beam welding of 6mm thick aluminum alloys

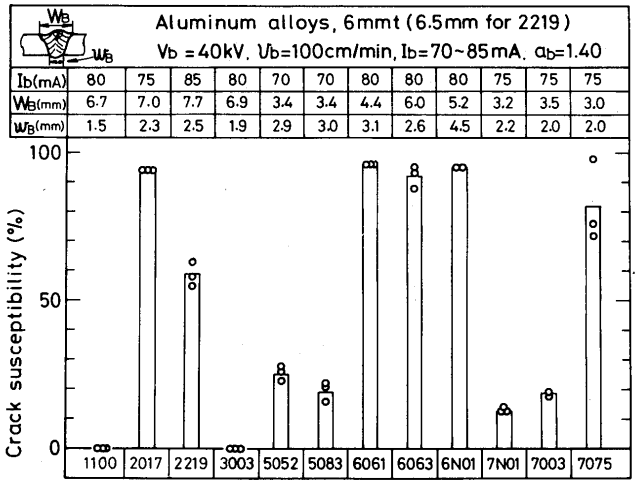

Fig. 7 Comparison of susceptibility to solidification crack for various aluminum alloys using the new specimen

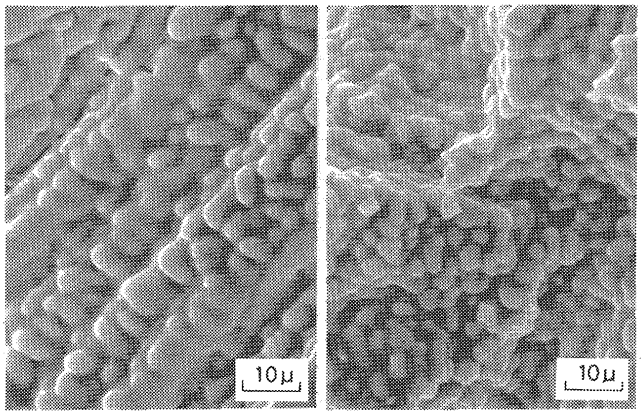

(a) 6061 alloy (b) 5083 alloy

Fig. 10 Typical fractographic appearance of specimen cracked

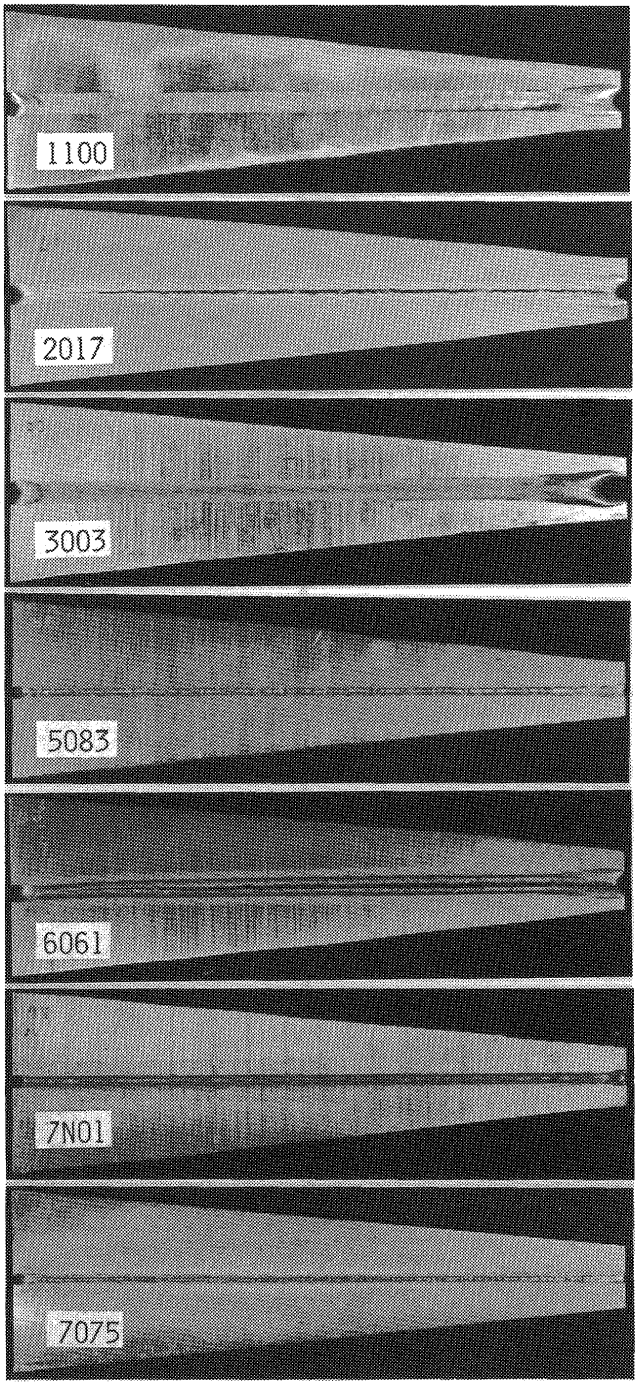

Fig. 8 Typical overall appearances of specimen tested

was also a little different depending upon the type of alloy, and widths of Al–Mg (5000 type) and Al–Zn–Mg (7000 type) alloys were narrower than those of the other types of alloy due to high vapor pressure of Mg and Zn in aluminum. Three data in crack susceptibility for each alloy were not so scattering.

The order of crack susceptibility for various alloys is considered to be reasonable judging from the viewpoint of practical experiences.

The typical appearances of overall specimen tested and the crosssectional weld bead are shown in **Fig.8** and **Fig.9** respectively. Typical fractographic observations of cracked surface are shown in **Fig.10** which present the appearance of solidification cracking.

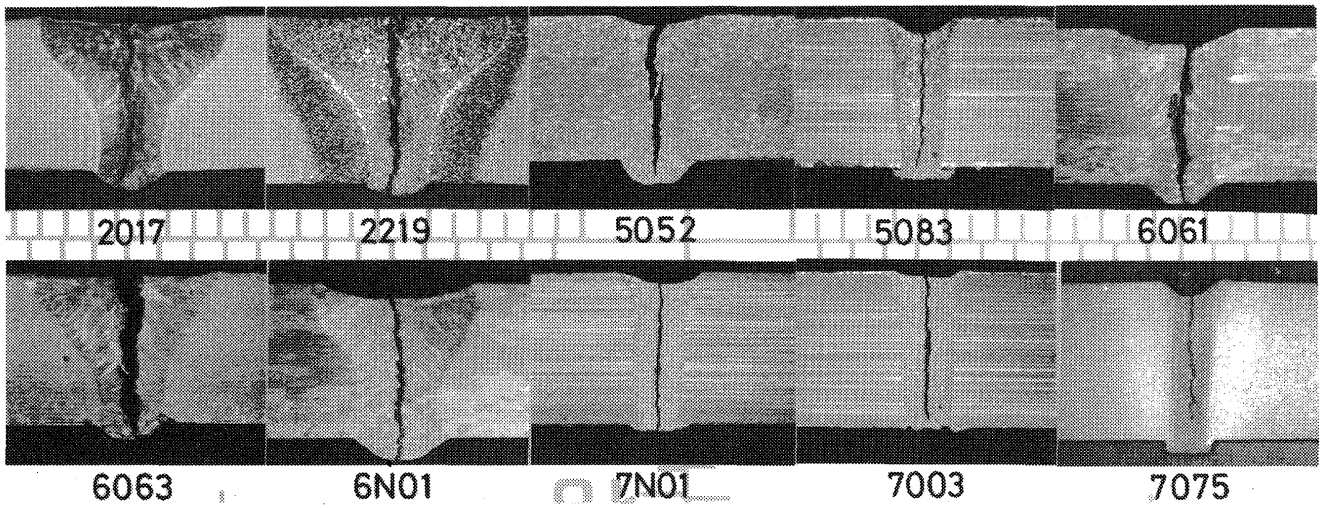

Fig. 9 Typical crosssectional bead of specimen cracked

4. Test Specimen for Austenitic Stainless Steels

4.1 Materials and welding procedure used

Austenitic stainless steels used were 3mm, partly 4mm thick commercial SUS(AISI) 310S, 316, 321 and 304 whose chemical compositions were shown in **Table 2.**

Table 2 Chemical compositions of commercial stainless steels used

Material	Chemical composition (wt%)									
	C	Si	Mn	P	S	Cr	Ni	Mo	Cu	Ti
SUS310S	0.07	1.04	1.46	0.012	0.005	25.48	19.53	0.05	0.02	-
SUS316	0.062	0.59	1.16	0.033	0.009	18.76	10.29	2.10	0.21	-
SUS321	0.058	0.84	1.19	0.034	0.016	17.54	9.46	0.22	0.13	0.34
SUS304	0.066	0.58	1.54	0.032	0.013	18.55	8.28	0.25	0.32	-

Electron-beam welding machine and procedure were almost the same as in 3.1 in aluminum alloys. However, as the specimen size in stainless shown in Fig.13 was much slender than in aluminum alloys, the test specimen was often self-moving due to heat expansion during electron-beam welding operation. Therefore the specimen was fixed to the fixture by two 3mm dia. bolts in 3.5mm dia. loose holes near the final edge of test specimen in advance of welding as shown in Fig.13. The crack susceptibility of the test specimen was not affected with the fixation.

4.2 Shape and dimension of test specimen

The decision of shape and dimension of test specimen was done with similar steps for aluminum alloys. As SUS 310S of fully austenitic stainless steel is the most susceptible to cracking in these four steels, the dimension of the test specimen were mainly decided with SUS310S. For decision of (1/2)**Ws** electron–beam welding condition of 40KV–100cm/min was applied for three different ab values of 1.0, 0.95 and 0.84 with respective beam current of 60, 80 and 100mA. The width of (1/2)**Ws** was changed as 5 to 10mm as shown in **Fig.11**. The wider the bead width, the more the susceptibility to crack in same (1/2)**Ws**. However there was no crack initiated in the narrowest bead with 1.0 of ab at 5mm of (1/2)**Ws**. It seems that the specimen width narrower than 5mm of (1/2)**Ws** is required to make crack initiation for the narrowest weld bead. Then the authors decided 8mm as **Ws** which was the minimum length at specimen edge for low voltage electron-beam welding in order to keep a steady weld start. If a choice of high voltage electron–beam welding is admitted, much narrow **Ws** will be recommended.

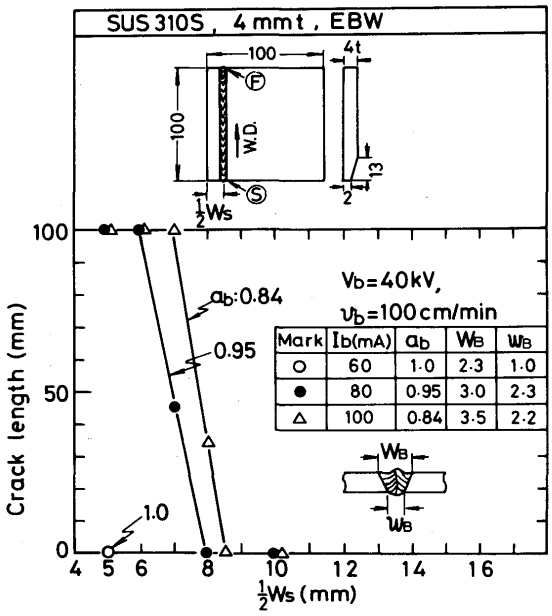

Fig. 11 Investigation of specimen width, (1/2)Ws,required to cause crack initiation and to keep crack propagation for stainless steel of 310S

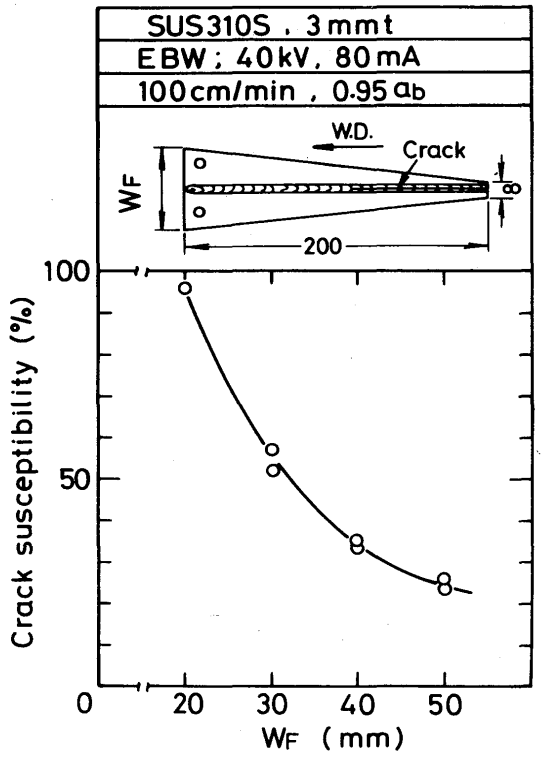

Fig. 12 Effect of width at the end of specimen, W_F, in specimen length of 200mm on crack susceptibility of weld bead for 310S

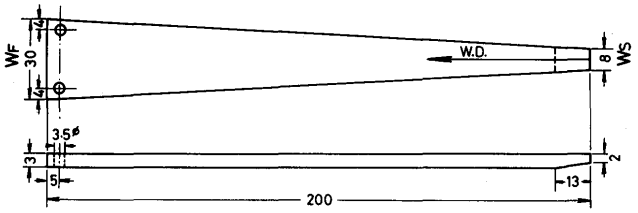

Fig. 13 A new crack susceptible test specimen recommended for electron–beam welding of 3mm thick stainless steels

Next, the decision of W_F was tried in 200mm in specimen length L as shown in **Fig.12.** As a result the W_F recommended was considered to be 30mm or a little less than 30mm. In consideration of much susceptible alloys W_F was decided for 30mm here. The final specimen shape and dimension are shown in **Fig.13.** The specimen is much slender than that of aluminum alloys, then is better to fix with bolts near the end of specimen as described in 4.1.

4.3 Comparion of crack susceptibility for various stainless steels

The crack susceptibility of four stainless steels SUS310S, 316,321 and 304 was compared in **Fig.14** using the test specimen shown in Fig.13. In Fig.14 the test specimen for 50mm in W_F was also tried to compare besides 30mm. Each three data in crack

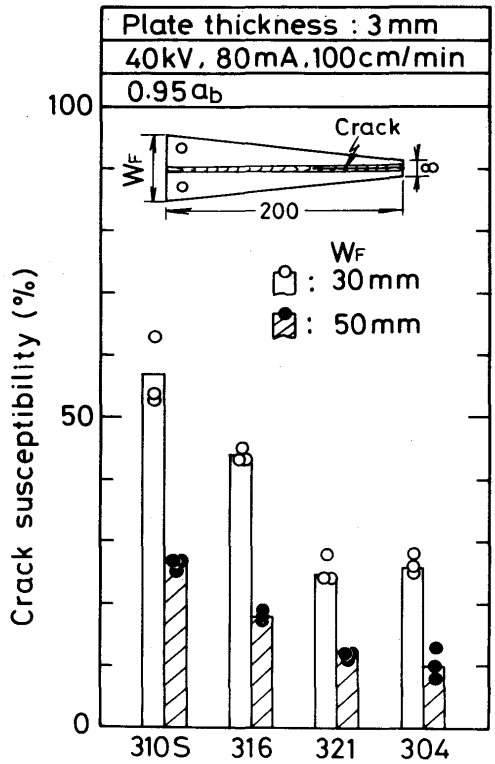

Fig. 14 Comparison of susceptibility to solidification crack for various stainless steels using the new test specimen

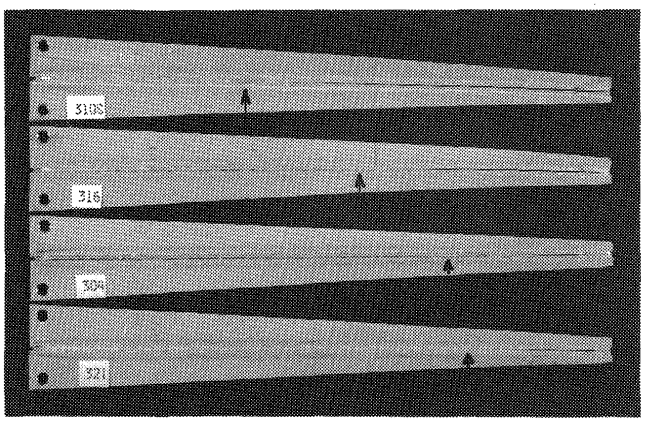

Fig. 15 Typical overall appearances of specimen tested

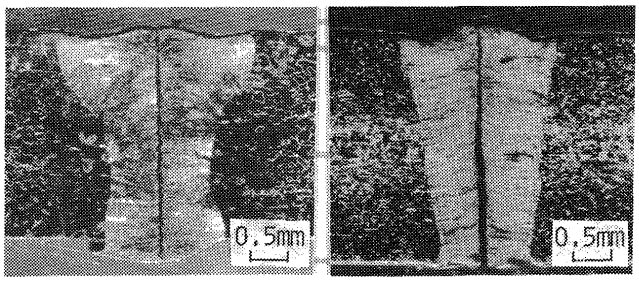

(a) 310S (b) 304

Fig. 16 Typical crosssectional bead of specimen cracked

susceptibility for four steels have a very narrow scattering and show a stable value. The order of crack

susceptibility for these four steels coincides well with practical experiences.

The typical appearance of the specimen tested is shown in **Fig.15** in which arrow mark indicates ceasing point of crack. Moreover typical crosssectional beads are shown in **Fig.16.** Also typical fractographic appearance of cracked surfaces is shown in **Fig.17** which shows solidification cracking.

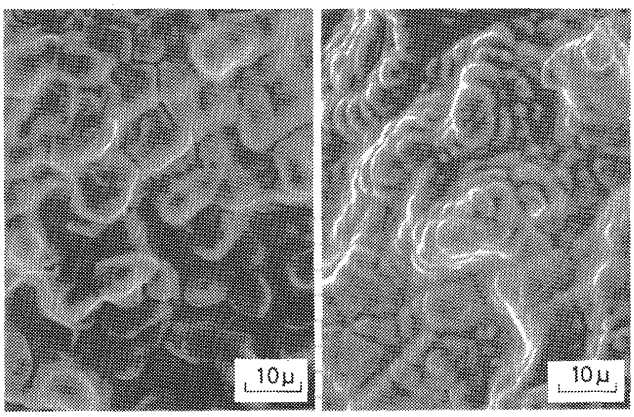

(a) 310S (b) 304

Fig. 17 Typical fractographic appearance of specimen cracked

5. Conclusions

The following conclusions were drawn for the development of the new self-restrained solidification cracking test specimen for electron-beam welding.

(1) The authors have qualitatively explained the desirable shape of test specimen which used for evaluation of solidificaion crack susceptibility of weld bead with higher welding speed in Houldcroft-type test, using the cracking mechnism in the previous investigations.

(2) In accordance with the consideration in (1), the dimensions of the new test specimen were experimentally decided for 6mm thick aluminum alloys and 3mm thick austenitic stainless steels, respectively, using electron-beam welding with 100cm/min of welding speed by Sciaky electron-beam welder. The specimens recommended for crack susceptible test are shown in Fig.6 for aluminum alloys and in Fig.13 for stainless steels.

(3) The susceptibility tests to solidification crack were done and compared for various 6mm thick aluminum alloys and 3mm thick stainless steels. The test results coincided well with that of practical experiences. Moreover the scattering of test data in these specimens was narrow enough.

Further investigations will be required if these new test specimens are useful for testing of thicker material, higher welding speed, other kinds of alloy and other types of electron-beam welder.

Acknowledgement

The authors wish to thank Dr. H. Irie and Mr. S. Tsukamoto of NRIM for their close cooperation for electron-beam welding operation of test specimens. The authors also wish to thank Mr. K. Tsukamoto, Showa Aluminum Corporation, and Mr. K. Saitoh, Nippon Stainless Steel Co., Ltd., for their supports for materials.

References

1) F. Matsuda, K. Nakata, S. Harada : Trans. JWRI, 9(1980) 2, 83–93.
2) F. Matsuda, K. Nakata : Trans. JWRI, 11(1982)1, 141–143.
3) P. T. Houldcroft : B.W.J., 2(1955) 10, 471–475.
4) J. H. Rogerson, B. Cotterel, J. C. Boreland : W.J., 42(1963)6, 264s–268s.
5) K. Ando et al : Report of JWS, 42(1973)9, 37–47(in Japanese)
6) T. Senda, F. Matsuda et al : Trans. JWS, 2(1971)2, 1–22.